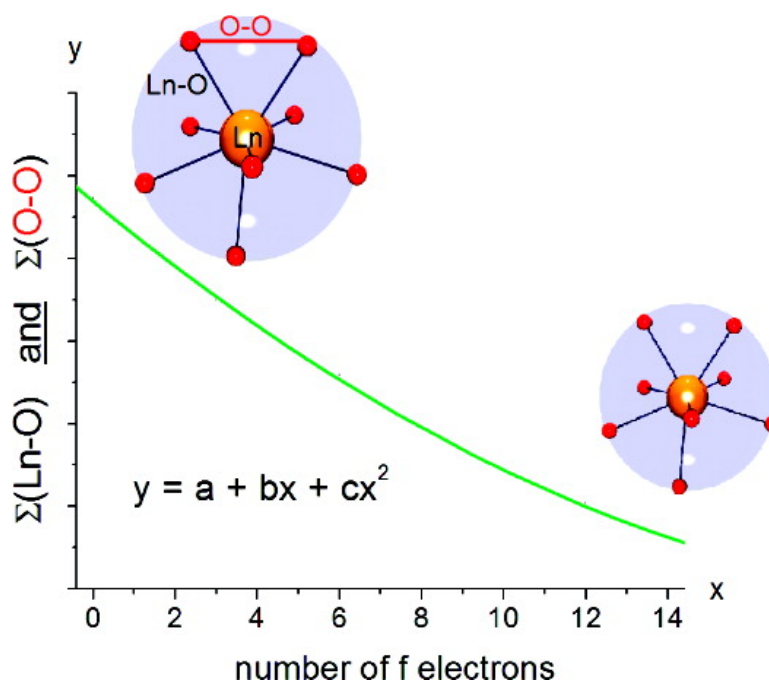


The Lanthanide Contraction Revisited

Michael Seitz, Allen G. Oliver, and Kenneth N. Raymond

J. Am. Chem. Soc., **2007**, 129 (36), 11153-11160 • DOI: 10.1021/ja072750f • Publication Date (Web): 18 August 2007

Downloaded from <http://pubs.acs.org> on February 14, 2009



More About This Article

Additional resources and features associated with this article are available within the HTML version:

- Supporting Information
- Links to the 10 articles that cite this article, as of the time of this article download
- Access to high resolution figures
- Links to articles and content related to this article
- Copyright permission to reproduce figures and/or text from this article

[View the Full Text HTML](#)



ACS Publications
 High quality. High impact.

The Lanthanide Contraction Revisited

Michael Seitz, Allen G. Oliver, and Kenneth N. Raymond*

Contribution from the Department of Chemistry, University of California,
Berkeley, California 94720-1460

Received April 19, 2007; E-mail: raymond@socrates.berkeley.edu

Abstract: A complete, isostructural series of complexes with La–Lu (except Pm) with the ligand TREN-1,2-HOIQO has been synthesized and structurally characterized by means of single-crystal X-ray analysis. All complexes are 1D-polymeric species in the solid state, with the lanthanide being in an eight-coordinate, distorted trigonal-dodecahedral environment with a donor set of eight unique oxygen atoms. This series constitutes the first complete set of isostructural complexes from La–Lu (without Pm) with a ligand of denticity greater than two. The geometric arrangement of the chelating moieties slightly deviates across the lanthanide series, as analyzed by a shape parameter metric based on the comparison of the dihedral angles along all edges of the coordination polyhedron. The apparent lanthanide contraction in the individual Ln–O bond lengths deviates considerably from the expected quadratic decrease that was found previously in a number of complexes with ligands of low denticity. The sum of all bond lengths around the trivalent metal cation, however, is more regular, showing an almost ideal quadratic behavior across the entire series. The quadratic nature of the lanthanide contraction is derived theoretically from Slater's model for the calculation of ionic radii. In addition, the sum of all distances along the edges of the coordination polyhedron show exactly the same quadratic dependence as the Ln–X bond lengths. The universal validity of this coordination sphere contraction, concomitant with the quadratic decrease in Ln–X bond lengths, was confirmed by reexamination of four other, previously published series of lanthanide complexes. Owing to the importance of multidentate ligands for the chelation of rare-earth metals, this result provides a significant advance for the prediction and rationalization of the geometric features of the corresponding lanthanide complexes, with great potential impact for all aspects of lanthanide coordination.

1. Introduction

The coordination chemistry of the lanthanides shows much structural diversity. However, there is often only a limited degree of predictability because of the absence of strong ligand field effects, resulting in small energetic differences between different geometric arrangements and/or coordination numbers. One of the few reliable cornerstones for the rationalization of geometric features around lanthanide cations is the well-known phenomenon of the lanthanide contraction.^{1,2} Recently, it has been shown that in this context the monotonic decrease of certain parameters, such as Ln–X (X = Lewis-basic donor), can be best described by a second-order polynomial. This dependence was established by the examination of isostructural series of lanthanide complexes published in the literature.³ Subsequently, this dependence has also been observed for a few other examples of incomplete series including solid-state materials,⁴ as well as

coordination compounds.⁵ Because of the rarity of isostructural series over the whole range from La to Lu (excluding Pm), only limited structural information is available for the further analysis of the lanthanide contraction and geometrical ramifications thereof. Specifically, for complexes with ligands of higher denticity, which are often most relevant for the application of lanthanides (e.g., luminescence,⁶ MRI,⁷ radioisotope labeling,⁸ etc.), no example of a complete isostructural series with La–Lu (without Pm) has been presented.⁹ We report here the first case of such a series of complexes with a multidentate ligand and a detailed analysis of the structural changes corresponding to the lanthanide contraction as seen here and in previous systems.

- (1) Goldschmidt, V. M.; Barth, T.; Lunde, G. *Skrifter Norske Videnskaps-Akademi i Oslo, I. Mat.-Naturv. Klasse* **1925**, *7*, 59.
- (2) (a) Shannon, R. D. *Acta Crystallogr. A* **1976**, *32*, 751. (b) Shannon, R. D.; Prewitt, C. T. *Acta Crystallogr. B* **1969**, *25*, 925. (c) Siekierski, S. *Pol. J. Chem.* **1992**, *66*, 215. (d) Siekierski, S. *Inorg. Chim. Acta* **1985**, *109*, 199. (e) Gerkin, R. E.; Reppart, W. J. *Acta Crystallogr. C* **1984**, *40*, 781–786. (f) Chatterjee, A.; Maslen, E. N.; Watson, K. J. *Acta Crystallogr. B* **1988**, *44*, 381–386.
- (3) Quadrelli, E. A. *Inorg. Chem.* **2002**, *41*, 167–169.
- (4) (a) Deng, B.; Ellis, D. E.; Ibers, J. A. *Inorg. Chem.* **2002**, *41*, 5716–5720. (b) Yao, J.; Deng, B.; Sherry, L. J.; McFarland, A. D.; Ellis, D. E.; Van, Duyne, R. P.; Ibers, J. A. *Inorg. Chem.* **2004**, *43*, 7735–7740.

- (5) (a) Baisch, U.; Belli Dell'Amico, D.; Calderazzo, F.; Conti, R.; Labella, L.; Marchetti, F.; Quadrelli, E. A. *Inorg. Chim. Acta* **2004**, *357*, 1538–1548. (b) Baisch, U.; Belli Dell'Amico, D.; Calderazzo, F.; Labella, L.; Marchetti, F.; Merigo, A. *Eur. J. Inorg. Chem.* **2004**, 1219–1224.
- (6) (a) Bünzli, J.-C. G. *Acc. Chem. Res.* **2006**, *39*, 53–61. (b) Bünzli, J.-C. G.; Piguët, C. *Chem. Soc. Rev.* **2005**, *34*, 1048–1077. (c) Parker, D. *Chem. Soc. Rev.* **2004**, *33*, 156–165.
- (7) (a) Caravan, P.; Ellison, J. J.; McMurry, T. J.; Lauffer, R. B. *Chem. Rev.* **1999**, *99*, 2293–2352. (b) Aime, S.; Botta, M.; Fasano, M.; Geninatti Crich, S.; Terreno, E. *Coord. Chem. Rev.* **1999**, *185–186*, 321–333. (c) *The Chemistry of Contrast Agents in Medical Magnetic Resonance Imaging*; Tóth, E., Helm, L., Merbach, A. E., Eds.; Wiley: Chichester, U.K., 2001. (d) Raymond, K. N.; Pierre, V. C. *Bioconjugate Chem.* **2005**, *16*, 3–8.
- (8) *Handbook of Radiopharmaceuticals. Radiochemistry and Applications*; Welch, M. J., Redvanly, C. S., Eds.; Wiley: Chichester, U.K., 2003.
- (9) Seitz, M.; Pluth, M. D.; Raymond, K. N. *Inorg. Chem.* **2007**, *46*, 351–353.

Scheme 1. Synthesis of Lanthanide Complexes with TREN-1,2-HOIQO

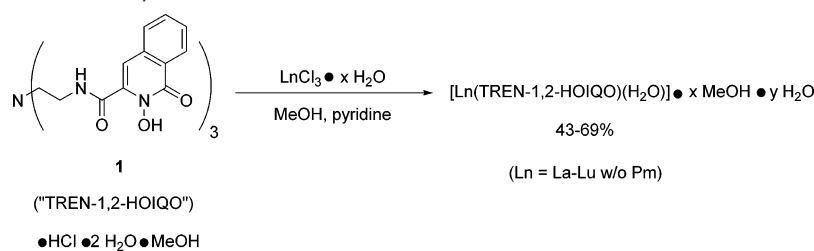


Table 1. Crystal Data for Lanthanide Complexes (La–Gd) with TREN-1,2-HOIQO (1)

	[La(1)(H ₂ O)]·H ₂ O	[Pr(1)(H ₂ O)]·H ₂ O	[Nd(1)(H ₂ O)]·H ₂ O	[Sm(1)(H ₂ O)]·H ₂ O	[Eu(1)(H ₂ O)]·H ₂ O	[Gd(1)(H ₂ O)]·H ₂ O
formula	C ₃₆ H ₃₄ LaN ₇ O ₁₁	C ₃₆ H ₃₄ N ₇ O ₁₁ Pr	C ₃₆ H ₃₄ N ₇ NdO ₁₁	C ₃₆ H ₃₄ N ₇ O ₁₁ Sm	C ₃₆ H ₃₄ EuN ₇ O ₁₁	C ₃₆ H ₃₄ GdN ₇ O ₁₁
mol. wt	879.61	881.61	884.94	891.05	892.66	897.95
cryst	colorless plate	red plate	red plate	red plate	colorless plate	colorless plate
appearance						
cryst syst	monoclinic	monoclinic	monoclinic	monoclinic	monoclinic	monoclinic
space group	<i>P</i> ₂ ₁ / <i>c</i>	<i>P</i> ₂ ₁ / <i>c</i>	<i>P</i> ₂ ₁ / <i>c</i>	<i>P</i> ₂ ₁ / <i>c</i>	<i>P</i> ₂ ₁ / <i>c</i>	<i>P</i> ₂ ₁ / <i>c</i>
<i>a</i> [Å]	12.3545(11)	12.3482(14)	12.355(5)	12.3528(13)	12.380(3)	12.3590(18)
<i>b</i> [Å]	26.745(2)	26.594(3)	26.521(5)	26.371(3)	26.314(5)	26.307(4)
<i>c</i> [Å]	10.6674(9)	10.6089(12)	10.605(5)	10.6066(11)	10.612(2)	10.5933(15)
α [deg]	90	90	90	90	90	90
β [deg]	97.018(2)	96.581(2)	96.512(5)	96.441(2)	96.470(4)	96.343(3)
γ [deg]	90	90	90	90	90	90
vol [Å ³]	3498.3 (5)	3460.9(7)	3452(2)	3433.3(6)	3435.0(12)	3423.1(9)
<i>Z</i>	4	4	4	4	4	4
ρ [g cm ⁻³]	1.67	1.69	1.70	1.72	1.73	1.74
μ [mm ⁻¹]	1.30	1.48	1.58	1.79	1.90	2.01
cryst size [mm ³]	0.24 × 0.22 × 0.09	0.27 × 0.13 × 0.09	0.30 × 0.15 × 0.08	0.28 × 0.13 × 0.06	0.15 × 0.07 × 0.04	0.19 × 0.13 × 0.06
temp [K]	160(2)	157(2)	156(2)	159(2)	158(2)	164(2)
radiation [Å]	Mo Kα (λ = 0.71073)	Mo Kα (λ = 0.71073)	Mo Kα (λ = 0.71073)	Mo Kα (λ = 0.71073)	Mo Kα (λ = 0.71073)	Mo Kα (λ = 0.71073)
θ max [deg]	26.40	26.37	26.39	26.40	26.42	26.42
measd reflns	19871	19631	19552	19446	19433	19276
independent reflns	7071	7016	6951	6953	6936	6861
reflns in ref	5080 (<i>I</i> ≥ 2σ(<i>I</i>))	4840 (<i>I</i> ≥ 2σ(<i>I</i>))	4620 (<i>I</i> ≥ 2σ(<i>I</i>))	4741 (<i>I</i> ≥ 2σ(<i>I</i>))	4280 (<i>I</i> ≥ 2σ(<i>I</i>))	4343 (<i>I</i> ≥ 2σ(<i>I</i>))
params	496	496	496	496	496	496
<i>R</i> ^a	0.0610	0.0507	0.0530	0.0483	0.0584	0.0564
<i>wR</i> ^b	0.1474	0.1086	0.1130	0.1042	0.1183	0.1138
<i>R</i> ^a (all data)	0.0897	0.0860	0.0951	0.0849	0.1120	0.1054
<i>wR</i> (all data)	0.1598	0.1194	0.1264	0.1148	0.1345	0.1285
GOF	1.050	1.035	1.030	1.026	1.008	1.003
Δρ _{max} [e/Å ³]	4.39 (near La)	1.01	1.48	1.39	1.36	1.85
Δρ _{min} [e/Å ³]	-0.14	-0.64	-0.86	-0.87	-0.75	-0.73

^a *R* factor definition: $R = \frac{\sum (||F_o| - |F_c||)}{\sum |F_o|}$. ^b SHELX-97 *wR* factor definition: $wR = \frac{[\sum w(F_o^2 - F_c^2)^2 / \sum w(F_o^2)]^{1/2}}$. Weighting scheme: $w = 1/[\sigma^2(F_o^2) + (np)^2]$, $p = [F_o^2 + 2F_c^2]/3$.

2. Results and Discussion

2.1. Complex Syntheses. We recently introduced the tripodal ligand TREN-1,2-HOIQO (**1**, Scheme 1) as a new ligand for iron(III) and lanthanide(III) cations (Ce, Eu, Gd, Lu).⁹ The lanthanide complexes were prepared as previously described by refluxing equimolar amounts of the ligand TREN-1,2-HOIQO and the corresponding lanthanide chloride (hydrated or anhydrous) in methanol with pyridine as the base (Scheme 1).

2.2. Crystal Structures. Single crystals of the resultant lanthanide complexes were grown by diffusion of water into solutions of the complexes in DMF. Unit-cell determinations and further analyses revealed that all structures crystallized in the monoclinic system *P*₂₁/*c* with very similar lattice parameters (Tables 1 and 2).

The structures were readily solved by direct methods. All the complexes are isostructural, with the same polymeric nature that was previously reported for the cerium complex of **1**.⁹ The ligand chelates the lanthanide in a heptadentate fashion through

three pairs of oxygen donors from the cyclic hydroxamic acid derivative 1,2-HOIQO and one bridging amide oxygen of a neighboring complex (Figure 1). The coordination sphere is completed by a water molecule to give an eight-coordinate lanthanide center with an approximately trigonal-faced dodecahedral geometry (vide infra).

2.3. Structural Analysis. 2.3.1. Isostructural Behavior. For the analysis of the lanthanide contraction and its ramifications, it is essential that the subjects of the study have the same or very similar structure to ensure that the nature of the lanthanide is the only changing parameter. In the literature on the lanthanide contraction to date, however, terms like “isostructural” and “isotypical” have been used in a rather qualitative fashion, although there have been some efforts to develop a more quantitative measure for the similarity of coordination compounds.¹¹ For the investigation of the present series of lanthanide

(10) ORTEP-3 for Windows: Farrugia, L. J. *J. Appl. Crystallogr.* **1997**, *30*, 565.

(11) Alvarez, S.; Alemany, P.; Casanova, D.; Cirera, J.; Lluell, M.; Avnir, D. *Coord. Chem. Rev.* **2005**, *249*, 1693–1708 and references cited therein.

Table 2. Crystal Data for Lanthanide Complexes (Tb–Lu) with TREN-1,2-HOIQO (1)

	Tb(1)(H ₂ O) ·H ₂ O	[Dy(1)(H ₂ O)] ·H ₂ O	[Ho(1)(H ₂ O)] ·H ₂ O	[Er(1)(H ₂ O)] ·H ₂ O	[Tm(1)(H ₂ O)] ·H ₂ O	[Yb(1)(H ₂ O)] ·H ₂ O	[Lu(1)(H ₂ O)] ·H ₂ O
formula	C ₃₆ H ₃₄ N ₇ O ₁₁ Tb	C ₃₆ H ₃₄ DyN ₇ O ₁₁	C ₃₆ H ₃₄ HoN ₇ O ₁₁	C ₃₆ H ₃₄ ErN ₇ O ₁₁	C ₃₆ H ₃₄ N ₇ O ₁₁ Tm	C ₃₆ H ₃₄ N ₇ O ₁₁ Yb	C ₃₆ H ₃₄ LuN ₇ O ₁₁
mol. wt	899.62	903.20	905.63	907.96	909.63	913.74	915.67
cryst appearance	yellow plate	colorless plate	colorless plate	colorless plate	colorless needle	red plate	colorless plate
cryst syst	monoclinic	monoclinic	monoclinic	monoclinic	monoclinic	monoclinic	monoclinic
space group	<i>P2₁/c</i>	<i>P2₁/c</i>	<i>P2₁/c</i>	<i>P2₁/c</i>	<i>P2₁/c</i>	<i>P2₁/c</i>	<i>P2₁/c</i>
<i>a</i> [Å]	12.3216(14)	12.3472(15)	12.345(2)	12.3589(18)	12.3920(13)	12.336(5)	12.417(2)
<i>b</i> [Å]	26.295(3)	26.188(3)	26.153(4)	26.132(4)	26.162(3)	26.006(10)	26.193(4)
<i>c</i> [Å]	10.5618(12)	10.5624(12)	10.5557(17)	10.5565(15)	10.5522(12)	10.546(4)	10.5619(17)
α [deg]	90	90	90	90	90	90	90
β [deg]	96.335(2)	96.220(2)	96.306(3)	96.277(2)	96.357(3)	96.443(5)	96.436(4)
γ [deg]	90	90	90	90	90	90	90
vol [Å ³]	3401.0(7)	3395.2(7)	3387.3(10)	3388.9(8)	3400.0(6)	3362(2)	3413.4(10)
<i>Z</i>	4	4	4	4	4	4	4
ρ [g cm ⁻³]	1.76	1.77	1.78	1.78	1.78	1.81	1.78
μ [mm ⁻¹]	2.16	2.23	2.41	2.55	3.21	2.86	3.56
cryst size [mm ³]	0.24 × 0.22 × 0.09	0.18 × 0.16 × 0.06	0.18 × 0.09 × 0.06	0.22 × 0.08 × 0.06	0.09 × 0.01 × 0.01	0.15 × 0.07 × 0.04	0.10 × 0.04 × 0.02
temp [K]	159(2)	162(2)	161(2)	165(2)	173(2)	158(2)	173(2)
radiation [Å]	Mo K α ($\lambda = 0.71073$)	Mo K α ($\lambda = 0.71073$)	Mo K α ($\lambda = 0.71073$)	Mo K α ($\lambda = 0.71073$)	synchro. ($\lambda = 0.7749$)	Mo K α ($\lambda = 0.71073$)	synchro. ($\lambda = 0.7749$)
θ max [deg]	26.40	26.45	26.39	26.39	29.19	26.44	25.62
meas reflns	19325	19202	19179	19114	35089	16284	20804
independent reflns	6901	6888	6833	6866	7007	6475	4946
reflns in ref	4833 ($I \geq 2\sigma(I)$)	5033 ($I \geq 2\sigma(I)$)	4390 ($I \geq 2\sigma(I)$)	4446 ($I \geq 2\sigma(I)$)	5731 ($I \geq 2\sigma(I)$)	3542 ($I \geq 2\sigma(I)$)	4578 ($I \geq 2\sigma(I)$)
params	496	496	496	496	496	496	496
<i>R</i> ^a	0.0517	0.0456	0.0551	0.0489	0.0474	0.0594	0.0313
<i>wR</i> ^b	0.1189	0.1027	0.1079	0.0986	0.1107	0.1059	0.0804
<i>R</i> ^a (all data)	0.0849	0.0725	0.1045	0.0976	0.0597	0.1432	0.0340
<i>wR</i> (all data)	0.1299	0.1121	0.1219	0.1118	0.1149	0.1312	0.0820
GOF	1.024	1.037	1.013	0.993	1.096	0.964	1.097
$\Delta\rho_{\max}$ [e/Å ³]	2.54	1.35	1.10	1.15	1.63	2.61	1.66
$\Delta\rho_{\min}$ [e/Å ³]	-0.84	-0.88	-0.93	-1.04	-1.97	-0.84	-0.73

^a *R* factor definition: $R = \sum(|F_o| - |F_c|) / \sum|F_o|$. ^b SHELX-97 *wR* factor definition: $wR = [\sum w(F_o^2 - F_c^2)^2 / \sum w(F_o^2)]^{1/2}$. Weighting scheme: $w = 1/[\sigma^2(F_o)^2 + (np)^2]$, $p = [F_o^2 + 2F_c^2]/3$.

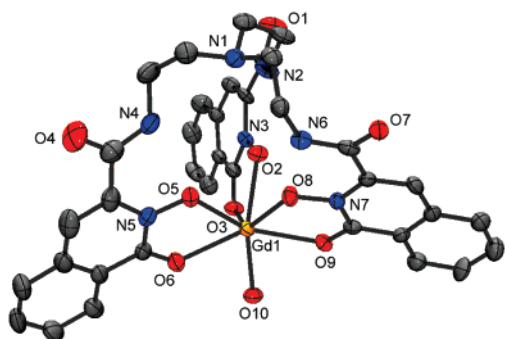


Figure 1. Asymmetric unit of [Gd(1)(H₂O)]·H₂O. Thermal ellipsoid plot (ORTEP-3 for Windows,¹⁰ 50% probability level) with atom numbering scheme. Hydrogens and the isolated water molecule are omitted for clarity. O7 is coordinated to a neighboring complex.

complexes, a shape-measure approach was utilized based on the dihedral angles along the edges of the coordination polyhedron¹² (Figure 2).

As the reference polyhedron the gadolinium complex was chosen due to the central position within the lanthanide series. Table 3 shows the dihedral angles of all complexes as well as the shape-measure deviation SM_{Gd} relative to this standard.

As can be seen in Table 3, the structures vary subtly with the dihedral angles varying by as much as ca. 5° (e.g., along

$$SM = \min \left[\sqrt{\frac{1}{m} \sum_{i=1}^m (\delta_i - \theta_i)^2} \right]$$

Figure 2. Shape measure *SM* with $\delta_i =$ observed dihedral angle along the *m* edges of a coordination polyhedron (angle between normals of adjacent faces) and $\theta_i =$ corresponding dihedral angle for a reference polyhedron.

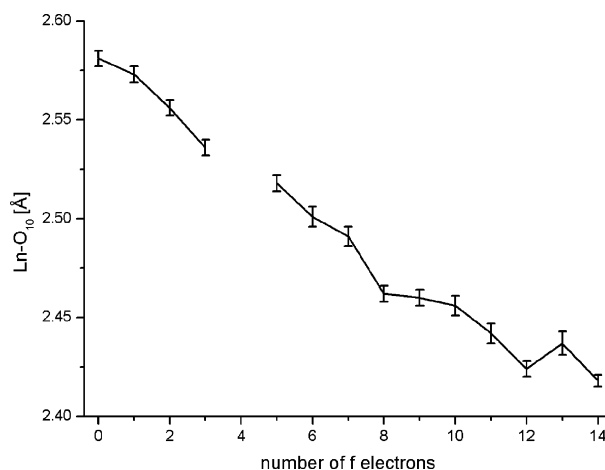


Figure 3. Decrease in Ln–O10 bond length in [Ln(1)(H₂O)] against the number of *f* electrons of the trivalent lanthanide cation.

edge O7–O8). On average, the differences are small as expressed by SM_{Gd} , which only shows a maximum variation of 1–2° for all complexes relative to the gadolinium species.

(12) (a) Xu, J.; Radkov, E.; Ziegler, M.; Raymond, K. N. *Inorg. Chem.* **2000**, *39*, 4156–4164. (b) Muetterties, E. L.; Guggenberger, L. J. *J. Am. Chem. Soc.* **1974**, *96*, 1748–1756. (c) Porai-Koshits, M. A.; Aslanov, L. A. *Zh. Strukt. Khim.* **1972**, *13*, 266.

Table 3. Dihedral Angles along the Edges of the Coordination Polyhedra [deg] of the Lanthanide Complexes with TREN-1,2-HOIQO (1)^a

edge	La	Ce ^b	Pr	Nd	Sm	Eu	Gd	Tb	Dy	Ho	Er	Tm	Yb	Lu
O7–O8	55.07	55.68	56.25	56.68	57.31	57.75	57.94	58.37	58.77	58.70	58.85	59.35	59.72	60.10
O7–O5	41.41	41.56	41.77	42.10	42.00	42.24	42.42	42.09	42.36	42.54	42.75	42.31	43.00	41.60
O7–O6	49.04	48.85	49.16	49.02	49.25	49.54	49.40	49.45	49.51	49.18	49.02	49.47	48.91	50.19
O7–O10	56.74	57.09	57.40	57.55	57.88	57.89	57.86	57.90	58.21	58.17	58.30	58.38	59.55	57.81
O7–O9	47.45	46.36	45.77	45.51	44.62	43.87	43.60	43.44	42.49	42.23	42.41	42.03	40.98	41.47
O6–O10	61.63	61.31	61.04	60.82	60.79	60.78	61.22	60.70	60.74	60.98	60.80	60.54	60.87	61.31
O9–O10	68.17	69.12	68.39	68.26	68.38	68.31	68.07	67.95	68.35	68.79	68.42	68.37	69.03	68.33
O3–O9	30.36	29.78	30.81	31.32	31.28	31.93	32.46	32.32	32.54	32.67	33.06	33.07	31.99	33.02
O2–O9	40.79	41.52	40.91	41.39	41.47	40.91	41.13	42.01	42.00	42.25	42.33	42.69	43.26	43.33
O2–O8	63.81	63.67	63.64	63.10	63.33	63.25	63.29	62.81	62.97	62.61	62.80	62.40	62.70	62.62
O2–O5	62.25	62.23	62.55	62.98	63.87	64.15	64.18	63.98	64.33	64.58	64.75	64.47	65.26	64.65
O3–O5	13.68	13.98	13.05	13.10	12.47	12.02	11.46	11.93	11.56	11.64	11.57	12.06	11.18	11.71
O2–O3	86.69	87.41	87.47	87.83	88.45	88.63	88.64	89.19	89.63	89.89	89.75	89.33	89.71	89.14
O5–O6	80.45	80.35	80.54	80.37	80.85	81.14	81.17	81.17	81.44	81.28	81.53	81.25	81.25	81.69
O3–O6	57.05	57.54	57.88	57.78	58.11	58.46	58.73	59.02	59.53	59.43	59.37	59.66	59.67	59.85
O10–O3	72.70	72.39	72.08	71.85	71.41	71.10	70.54	70.02	69.50	69.50	69.21	68.65	68.80	67.86
O9–O8	68.95	68.61	68.48	67.87	67.32	67.16	67.06	66.82	66.48	66.52	66.14	66.11	65.35	65.52
O8–O5	57.52	57.45	57.87	57.78	57.83	57.87	57.83	58.56	58.19	58.03	57.95	58.62	57.91	58.68
SM _{Gd}	2.01	1.78	1.44	1.24	0.89	0.70	0	0.65	0.69	0.72	0.74	0.94	1.27	1.26

^a Shape measure SM_{Gd} (deviation relative to the gadolinium complex). ^b Reference 9.

Table 4. Bond Lengths Ln–O in Lanthanide Complexes with TREN-1,2-HOIQO (1)

f electrons (Ln ³⁺)	d _{Ln–O3} (σ) [Å]	d _{Ln–O6} (σ) [Å]	d _{Ln–O9} (σ) [Å]	d _{Ln–O2} (σ) [Å]	d _{Ln–O5} (σ) [Å]	d _{Ln–O8} (σ) [Å]	d _{Ln–O10} (σ) [Å]	d _{Ln–O7} (σ) [Å]	Σd _{Ln–O} (σ) [Å]
0 (La)	2.482(4)	2.463(4)	2.479(4)	2.447(4)	2.443(5)	2.473(4)	2.581(4)	2.516(4)	19.884(34)
1 (Ce) ^a	2.469(4)	2.445(4)	2.450(4)	2.432(4)	2.426(4)	2.445(4)	2.573(4)	2.478(4)	19.718(32)
2 (Pr)	2.452(4)	2.427(4)	2.428(4)	2.407(4)	2.405(4)	2.437(3)	2.556(4)	2.473(4)	19.585(31)
3 (Nd)	2.434(4)	2.397(4)	2.415(4)	2.395(4)	2.394(4)	2.418(4)	2.536(4)	2.461(4)	19.450(32)
4 (Pm)									
5 (Sm)	2.396(4)	2.381(4)	2.374(4)	2.377(4)	2.377(4)	2.396(4)	2.518(4)	2.434(4)	19.253(32)
6 (Eu)	2.384(5)	2.368(5)	2.356(5)	2.361(5)	2.367(5)	2.386(5)	2.501(5)	2.420(5)	19.143(40)
7 (Gd)	2.373(5)	2.357(5)	2.349(5)	2.352(4)	2.343(5)	2.376(4)	2.491(5)	2.403(5)	19.044(38)
8 (Tb)	2.356(4)	2.338(4)	2.333(4)	2.336(4)	2.332(4)	2.361(4)	2.462(4)	2.381(4)	18.899(32)
9 (Dy)	2.340(4)	2.335(4)	2.322(4)	2.329(4)	2.327(4)	2.355(4)	2.460(4)	2.375(4)	18.843(32)
10 (Ho)	2.327(5)	2.318(5)	2.313(5)	2.312(5)	2.311(5)	2.333(5)	2.456(5)	2.353(5)	18.723(40)
11 (Er)	2.314(4)	2.309(5)	2.307(4)	2.307(4)	2.313(4)	2.330(4)	2.442(5)	2.353(4)	18.675(34)
12 (Tm)	2.308(4)	2.300(4)	2.294(4)	2.297(4)	2.304(4)	2.324(4)	2.424(4)	2.338(4)	18.589(32)
13 (Yb)	2.277(6)	2.282(6)	2.265(6)	2.300(6)	2.286(6)	2.301(6)	2.437(6)	2.333(6)	18.481(48)
14 (Lu)	2.288(3)	2.292(3)	2.282(3)	2.294(3)	2.287(3)	2.320(3)	2.418(3)	2.329(3)	18.510(24)
d _{La} /d _{Lu}	1.085	1.075	1.086	1.067	1.068	1.066	1.067	1.080	1.074

^a Reference 9.

The reasons for these deviations are not obvious but could be related to small ligand field effects or geometrical constraints imposed by the multidentate ligand (vide infra).

2.3.2. Ln–O Bond Lengths. As the next step, the decrease in Ln–O bond lengths was analyzed as evidence for the lanthanide contraction. In the complexes with TREN-1,2-HOIQO, all eight Ln–O bonds are different from each other, providing a rich source of structural data. Each bond length decreases by approximately 7–8% going from La to Lu in accordance with typical values for the lanthanide contraction (Table 4).

While the general trend of decreasing distances with heavier lanthanide is seen in every case, the individual classes of bond lengths cannot be fit by a second-order polynomial as was proposed.³ Figure 3 shows as an example the dependence of the bond length Ln–O10.¹³ In effect, the force field of the ligand responds to the change in the average metal ion size to distribute the metal–ligand bond-length changes, more in some and less in others. However the sum of all bond lengths Ln–O averages out these deviations and hence shows the expected even

contraction.¹⁴ The data shown in Figure 4, were well fit by a weighted polynomial regression (with a weighting factor of σ^{-2} , $R^2 = 0.9978$).¹⁵

That the lanthanide contraction follows a quadratic decay has been experimentally established by others,³ but this dependence has not been derived from a theoretical model. The general reason for the decrease in ionic radii with higher atomic number is well-known to be the increase in effective nuclear charge owing to incomplete shielding of the (5s, 5p) electrons from the increased nuclear charge by the 4f electrons. This phenomenon can be treated with the theoretical model that was introduced by Slater¹⁶ and later modified by others.¹⁷ That model utilizes a set of empirical rules for the shielding of the nuclear charge Z from electrons in a particular orbital by inner electron shells, expressed by a screening constant s . The atomic or ionic radius in the Slater model is at the maximum of the radial part of the outermost orbital which has the analytical

(14) An equivalent alternative description would be the average bond length.

(15) σ = standard deviation.

(16) Slater, J. C. *Phys. Rev.* **1930**, *36*, 57–64.

(17) (a) Clementi, E.; Raimondi, D. L. *J. Chem. Phys.* **1963**, *38*, 2686–2689. (b) Clementi, E.; Raimondi, D. L.; Reinhardt, W. P. *J. Chem. Phys.* **1967**, *47*, 1300–1307.

(13) For more details see the Supporting Information.

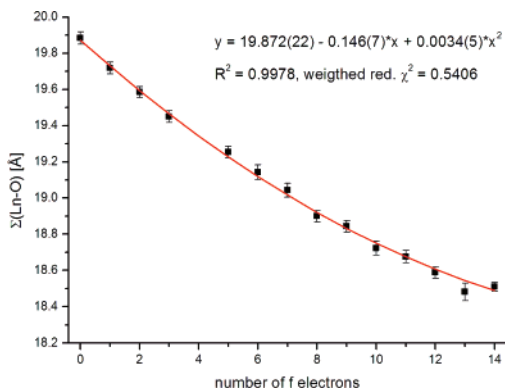


Figure 4. The sum of the Ln–O bond lengths against the number of f electrons. Quadratic fit in red (χ^2 -weighting factor: σ^{-2}).

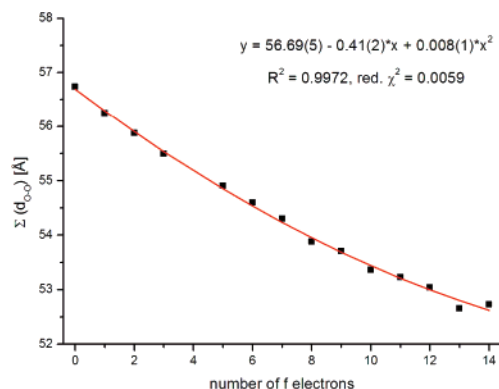


Figure 5. The sum of the O–O distances against the number of f electrons. Quadratic fit in red.

form

$$R(r) = (2\xi)^{n+1/2} [(2n)!]^{-1/2} r^{n-1} e^{-\xi r} \quad (1)$$

(with $\xi = (Z - s)/n^*$ and where n is the principal quantum number, s is the screening constant, and n^* is the effective quantum number.)

The maximum of this function is at

$$r_{\max} = \frac{n-1}{\xi} = \frac{(n-1)n^*}{Z-s} \quad (2)$$

To get the dependence of the ionic radius r_{\max} with the number of 4f electrons, the expressions $s = s_0 + kx$ and $Z = Z_0 + x$ (where s_0 is the screening constant for La^{3+} , k is the screening constant for one 4f electron, x is the number of 4f electrons, and $Z_0 = 57$ is the nuclear charge of La) are substituted in eq 2.

$$r(x) = r_{\max}(x) = \frac{n-1}{\xi} = \frac{(n-1)n^*}{Z_0 + x - s} = \frac{(n-1)n^*}{Z_0 + x - s_0 - kx} = \frac{(n-1)n^*}{Z_0^* + x(1-k)} \quad (3)$$

In addition, the value for the ionic radius of La^{3+} ($x = 0$) is

$$r_0 = r_{\max}(x=0) = \frac{(n-1)n^*}{Z_0^*} \quad (4)$$

From eqs 3 and 4, it follows that

$$r(x) = r_0 \frac{Z_0^*}{Z_0^* + x(1-k)} \quad (5)$$

Development of the corresponding Taylor series and termination after the third term gives an approximation for $r(x)$:

$$r(x) = \sum_{n=0}^{\infty} \left(\frac{x^n}{n!} \frac{d^n r(x=0)}{dx^n} \right) \approx r_0 - \frac{r_0(1-k)}{Z_0^*} x + \frac{r_0(1-k)^2}{(Z_0^*)^2} x^2 \quad (6)$$

The sum $S(x)$ over all m Ln–X bond lengths can be written as the sum of all lanthanide ionic radii $r(x)$ and all radii $r_{L,i}(x)$ of the ligating atoms:

$$S(x) = \sum_{i=1}^m r_{L,i}(x) + \sum_{i=1}^m r_i(x) = \sum_{i=1}^m r_{L,i}(x) + mr(x) \quad (7)$$

With the assumption that $\sum_{i=1}^m r_{L,i}(x) = S_L = \text{constant}$, the sum in eq 7 can be rewritten as

$$S(x) = S_L + mr(x) = S_L + mr_0 - \frac{mr_0(1-k)}{Z_0^*} x + \frac{mr_0(1-k)^2}{(Z_0^*)^2} x^2 = a + bx + cx^2 \quad (8)$$

with

$$a = S_L + mr_0; \quad b = -\frac{mr_0(1-k)}{Z_0^*}; \quad c = \frac{mr_0(1-k)^2}{(Z_0^*)^2} \quad (9)$$

From the eqs 9, the screening constant can be determined by the following relationship:

$$\frac{c}{b} = -\frac{(1-k)}{Z_0^*} \quad (10)$$

$$k = 1 + Z_0^* \frac{c}{b} \quad (11)$$

Calculating k with the measured parameters c and b (Figure 4) of the present lanthanide series and a value for $Z_0^* = 15.42$ (5p electrons¹⁷) yields

$$k = 0.64 \quad (12)$$

The good agreement with the commonly accepted value for the screening constant of $k = 0.69$ for f electrons shows the validity of the presented model.

2.3.3. O–O Bond Lengths. Most of the investigations reported so far in the literature are limited to the analysis of the Ln–X bond lengths. However, for multidentate ligands there is a considerable constraint on the coordination geometry that must be addressed. To assess the behavior of the ligand in this respect, the change in the distances between the eight coordinating donor atoms was investigated (Table 5).

Some features seen in the data are (1) unlike the Ln–O bond lengths, the decrease in O–O distances is not uniformly

Table 5. Distances O–O between Coordinating O Donors in Lanthanide Complexes with TREN-1,2-HOIQO (1)

f electrons (Ln ³⁺)	d _{07–09} [Å]	d _{03–05} [Å]	d _{07–05} [Å]	d _{03–09} [Å]	d _{05–06} [Å]	d _{09–010} [Å]	d _{02–03} [Å]	d _{07–08} [Å]	d _{07–010} [Å]	d _{03–06} [Å]
0 (La)	3.120	3.942	3.408	3.960	2.568	3.213	2.557	3.078	3.124	3.284
1 (Ce) ^a	3.109	3.902	3.379	3.912	2.555	3.159	2.562	3.043	3.104	3.224
2 (Pr)	3.112	3.908	3.353	3.840	2.557	3.119	2.551	3.039	3.086	3.217
3 (Nd)	3.112	3.897	3.335	3.793	2.551	3.086	2.549	3.006	3.072	3.190
4 (Pm)										
5 (Sm)	3.085	3.865	3.319	3.703	2.562	3.023	2.567	2.986	3.040	3.135
6 (Eu)	3.083	3.866	3.294	3.646	2.560	2.976	2.551	2.967	3.031	3.137
7 (Gd)	3.085	3.852	3.258	3.610	2.562	2.973	2.546	2.953	3.015	3.120
8 (Tb)	3.067	3.823	3.253	3.578	2.556	2.936	2.534	2.928	2.976	3.074
9 (Dy)	3.074	3.817	3.237	3.535	2.558	2.901	2.544	2.918	2.969	3.063
10 (Ho)	3.061	3.795	3.208	3.515	2.552	2.891	2.539	2.884	2.959	3.033
11 (Er)	3.060	3.792	3.211	3.489	2.544	2.876	2.549	2.884	2.948	3.018
12 (Tm)	3.059	3.775	3.217	3.470	2.562	2.854	2.538	2.881	2.924	2.998
13 (Yb)	3.042	3.738	3.188	3.412	2.542	2.824	2.521	2.856	2.920	2.958
14 (Lu)	3.054	3.752	3.194	3.417	2.552	2.831	2.535	2.860	2.913	2.974
d _{La} /d _{Lu}	1.022	1.051	1.067	1.159	1.006	1.135	1.009	1.076	1.072	1.104

f electrons (Ln ³⁺)	d _{07–06} [Å]	d _{010–03} [Å]	d _{02–05} [Å]	d _{02–09} [Å]	d _{09–08} [Å]	d _{08–05} [Å]	d _{06–010} [Å]	d _{02–08} [Å]	Σd _{0–0} [Å]
0 (La)	3.143	3.092	3.158	3.602	2.576	3.090	2.905	2.915	56.735
1 (Ce) ^a	3.122	3.064	3.128	3.555	2.574	3.065	2.907	2.881	56.245
2 (Pr)	3.100	3.023	3.106	3.509	2.576	3.031	2.884	2.862	55.873
3 (Nd)	3.077	2.992	3.086	3.477	2.576	2.997	2.856	2.843	55.495
4 (Pm)									
5 (Sm)	3.054	2.931	3.040	3.428	2.573	2.959	2.839	2.795	54.904
6 (Eu)	3.038	2.910	3.023	3.392	2.570	2.940	2.838	2.775	54.597
7 (Gd)	3.023	2.888	3.012	3.363	2.565	2.914	2.804	2.758	54.301
8 (Tb)	3.004	2.850	2.995	3.326	2.567	2.890	2.774	2.749	53.880
9 (Dy)	3.001	2.842	2.984	3.302	2.570	2.881	2.788	2.724	53.708
10 (Ho)	2.977	2.826	2.955	3.284	2.558	2.855	2.767	2.702	53.361
11 (Er)	2.976	2.802	2.953	3.272	2.564	2.853	2.753	2.684	53.228
12 (Tm)	2.966	2.792	2.933	3.248	2.572	2.835	2.736	2.682	53.042
13 (Yb)	2.954	2.788	2.927	3.221	2.544	2.809	2.741	2.669	52.654
14 (Lu)	2.956	2.761	2.928	3.216	2.579	2.812	2.722	2.674	52.730
d _{La} /d _{Lu}	1.063	1.120	1.079	1.120	0.999	1.090	1.067	1.090	1.076

^a Reference 9.**Table 6.** Absolute and Normalized Parameters of the Quadratic Fits ($y = a + bx + cx^2$) for the Lanthanide (Ln–X) and the Coordination Sphere (X–X) Contraction of the Series of Lanthanide Complexes (X = N, O)

entry	series	a (σ)	b (σ)	c (σ)	R ²	normalized a* (a* = a/a)	normalized b* (b* = b/a)	normalized c* (c* = c/a)
1a	[Ln(H ₂ O) ₉](EtOSO ₃) ₃ (Ln–O)	22.912(11)	–0.1562(38)	0.00347(28)	0.9979	1	–0.0068	0.00015
1b	[Ln(H ₂ O) ₉](EtOSO ₃) ₃ (O–O)	64.082(49)	–0.434(16)	0.0091(11)	0.9978	1	–0.0068	0.00014
2a	[Ln(TREN–SAL)] (Ln–X)	17.620(24)	–0.107(8)	0.00165(56)	0.9955	1	–0.0061	0.00009
2b	[Ln(TREN–SAL)] (X–X)	50.416(70)	–0.261(23)	0.0016(17)	0.9953	1	–0.0052	0.00003
3a	[Ln(TREN–1,2–HOIQO)(H ₂ O)] (Ln–O)	19.872(22)	–0.146(7)	0.0034(5)	0.9978	1	–0.0073	0.00017
3b	[Ln(TREN–1,2–HOIQO)(H ₂ O)] (O–O)	56.69(5)	–0.411(17)	0.0086(12)	0.9972	1	–0.0072	0.00015
4a	[Ln(PhMeCH–DOTAM)(H ₂ O)](OTf) ₃ (Ln–X)	23.349(26)	–0.144(7)	0.00347(44)	0.9978	1	–0.0062	0.00015
4b	[Ln(PhMeCH–DOTAM)(H ₂ O)](OTf) ₃ (X–X)	61.17(10)	–0.376(29)	0.0088(17)	0.9951	1	–0.0061	0.00015
5a	[Ln(tptz)(NO ₃) ₃ (H ₂ O)] (Ln–X)	26.140(11)	–0.1801(43)	0.00452(35)	0.9993	1	–0.0069	0.00017
5b	[Ln(tptz)(NO ₃) ₃ (H ₂ O)] (X–X)	61.106(34)	–0.428(12)	0.00109(9)	0.9988	1	–0.0070	0.00018

distributed. While the three rigid hydroxamate moieties (O2–O3, O5–O6, and O8–O9) remain nearly unchanged, the rest of the distances vary greatly (between 1 and 16%). The average, however, as seen in the sum of all O–O distances, decreases by 7.6% and agrees well with the values of 7–8% for the shortening of the unconstrained Ln–O bond lengths in [Ln(1)-(H₂O)] (see section 2.3.2). (2) Similar to the trends seen in Ln–O and, presumably for the same reason, the decrease cannot be fit uniformly in other classes of O–O distances.¹³ Again however, the quadratic nature of the lanthanide contraction can be seen in the averaged O–O distances (Figure 5).

2.3.4. Generality. The observation that the sum of either the Ln–O bond lengths or the O–O distances shows an almost

perfect quadratic decrease in complexes with a multidentate ligand like TREN-1,2-HOIQO prompted us to compare these results with previously published sets of lanthanide complexes to see whether this phenomenon has general applicability. The following published series of lanthanide complexes were analyzed: (1) [Ln(H₂O)₉](EtOSO₃)₃ (highest denticity (HD) = 1, coordination number (CN) = 9);^{2c} (2) [Ln(TREN–SAL)] (HD = 7, CN = 7);¹⁸ (3) the present complexes [Ln(TREN–1,2–HOIQO)(H₂O)] (HD = 7, CN = 8); (4) [Ln(PhMeCH–

(18) (a) Kanesato, M.; Yokoyama, Y. *Chem. Lett.* **1999**, 137–138. (b) Kanesato, M.; Yokoyama, Y. *Anal. Sci.* **2000**, *16*, 335–336. (c) Bernhardt, P. V.; Flanagan, B. M.; Riley, M. J. *Aust. J. Chem.* **2000**, *53*, 229–231. (d) Bernhardt, P. V.; Flanagan, B. M.; Riley, M. J. *Aust. J. Chem.* **2001**, *54*, 229–232.

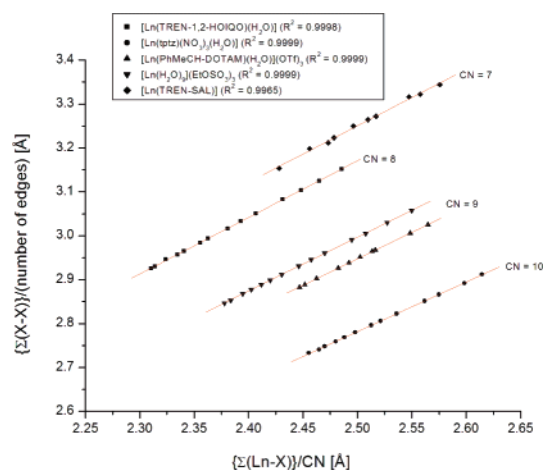


Figure 6. The average distance $X-X$ ($X = N, O$; bound to Ln) against the average $Ln-X$ ($X = N, O$) bond length for five series of isostructural lanthanide complexes. Linear fits in red.

DOTAM)(H₂O)](OTf)₃ (HD = 8, CN = 9);¹⁹ (5) [Ln(tptz)-(NO₃)₂(H₂O)] (HD = 3, CN = 10).²⁰ These were chosen for several reasons. First, each series has at least ten members of structurally characterized members. Second, series no. 2–5 feature multidentate ligands with medium to high denticities (HD = {3,7,7,8}), different coordination numbers (CN = {7,8,9,10}), and include the most important coordinating atoms for lanthanide coordination (a variety of N and O donors, neutral and anionic). Third, series no. 1 (with only monodentate aqua ligands) functions as a prototype for an unconstrained coordination environment. In addition, it represents the only other complete series of structurally characterized lanthanide complexes.

These literature examples were subjected to the same analysis as just described. The findings are essentially the same as described in these sections, with small additional features: (1) The series [Ln(H₂O)₉](EtOSO₃)₃ was used previously to establish the quadratic decrease in $Ln-X$ ($X = O$).³ In contrast, the complexes with multidentate ligands do not display this dependence in different classes of bond lengths $Ln-X$ ($X = N, O$) or nonbonded distances $X-X$ ($X = N, O$). (2) However the average $Ln-X$ ($X = N, O$) and $X-X$ ($X = N, O$) shows the expected quadratic behavior in all cases (Table 6).¹³

To be able to compare the different series with each other, the fit functions ($y = a + bx + cx^2$) were normalized by scaling the parameters by $1/a$ (Table 6, three columns on right). The normalized fits show common behavior: In four cases (entries 1, 3–5), the two normalized fits for $\Sigma(Ln-X)$ (entries a) and the corresponding $\Sigma(X-X)$ (entries b) are identical within error. Furthermore, the values for a , b , and c are very similar, but show some specificity for a particular ligand. Only for the complexes [Ln(TREN-SAL)] (entries 2a and b), do the values differ more, but are still nearly within error limits.

In addition, the relationship between average bond length ($\{\Sigma(Ln-X)\}/CN$) and average distance $X-X$ ($\{\Sigma(X-X)\}/\text{number}$

of edges of the coordination polyhedron) was analyzed as a different representation of the phenomenon summarized in Table 6 (Figure 6).¹³

Figure 6 clearly shows the almost perfect linearity in every case, grouped according to their coordination number. Taken together, these results show that the shortening in $Ln-X$ bond lengths is accompanied by a shrinking of the coordination sphere around the lanthanide that follows the same normalized quadratic decrease. However, this does not describe fully the situation for multidentate ligands because of the constraints in intraligand distances and angles of such ligands. Some donor–donor distances are constrained (e.g., the three bidentate hydroxamate moieties in TREN-1,2-HOIQO) and do not change at all or only very slightly with decreasing $Ln-X$ bond length. This results in greater changes for softer ligand deformations. The wide variation of the extent to which, for example, the individual O–O distances in [Ln(TREN-1,2-HOIQO)(H₂O)] (Table 5, last row) decrease over the lanthanide series (1–16%) illustrates this phenomenon.

3. Conclusion

In the course of this investigation we have shown that (1) [Ln(TREN-1,2-HOIQO)(H₂O)] represents the first complete set of isostructural complexes from La–Lu (without Pm) with a multidentate ligand and (2) a quadratic decrease is seen in the sum of all distances $Ln-X$ ($X = N, O$), even in complexes with multidentate ligands. This decrease is modeled successfully by Slater's model for calculating ionic radii. This result provides a rational analysis and prediction of the geometric features of multidentate ligands for the chelation of rare-earth metals.

4. Experimental Section

4.1. General. The lanthanide chlorides were purchased from commercial suppliers and used as received. The methanol used for the preparation of the metal complexes was HPLC-grade. Pyridine was distilled before use. DMF for the crystallizations was spectrophotometric grade. The elemental analyses were performed in duplicates by the microanalytical facility of the University of California, Berkeley. The syntheses and the analytical data for the ligand TREN-1,2-HOIQO, as well as for the cerium, europium, gadolinium, and lutetium complexes were reported previously.⁹

4.2. Synthesis of the Lanthanide Complexes. General Procedure for Complex Formation. Under argon, a solution of TREN-1,2-HOIQO (1.0 equiv) in MeOH was treated with solid LnCl₃·6H₂O (1.0 equiv) or LnCl₃ (anhydrous) (1.0 equiv), followed by pyridine and heated to reflux overnight. The resulting fine suspension was cooled to ambient temperature, and the precipitate was collected on a filter and washed with MeOH. After drying in vacuo at 50 °C (bath temp) for 6 h, the lanthanide complexes [Ln(TREN-1,2-HOIQO)(H₂O)]·xMeOH·yH₂O were obtained in analytically pure form as powders that were soluble in DMF, DMSO, and, only sparingly, in MeOH.

La: Starting with LaCl₃·6H₂O (9.1 mg, 37 μmol, 1.0 equiv), TREN-1,2-HOIQO·HCl·2H₂O·MeOH (30 mg, 37 μmol, 1.0 equiv), pyridine (62 mg) in 6 mL of MeOH gave 19 mg (55%) complex: mp > 300 °C. Anal. Calcd for C₃₆H₃₂LaN₇O₁₀·MeOH·2H₂O ($M_r = 929.66$): C, 47.80; H, 4.34; N, 10.55. Found: C, 47.62; H, 3.92; N, 10.49.

Pr: Starting with PrCl₃·6H₂O (14 mg, 40 μmol, 1.0 equiv), TREN-1,2-HOIQO·HCl·2H₂O·MeOH (33 mg, 40 μmol, 1.0 equiv), pyridine (62 mg) in 6 mL of MeOH gave 20 mg (55%) complex: mp > 300 °C. Anal. Calcd for C₃₆H₃₂N₇O₁₀Pr·MeOH ($M_r = 895.64$): C, 49.62; H, 4.05; N, 10.95. Found: C, 49.29; H, 3.78; N, 10.80.

Nd: Starting with NdCl₃·6H₂O (13.7 mg, 38.2 μmol, 1.0 equiv), TREN-1,2-HOIQO·HCl·2H₂O·MeOH (31.0 mg, 38.2 μmol, 1.0 equiv),

(19) (a) Batsanov, A. S.; Beeby, A.; Bruce, J. I.; Howard, J. A. K.; Kenwright, A. M.; Parker, D. *Chem. Commun.* **1999**, 1011–1012. (b) Aime, S.; Barge, A.; Batsanov, A. S.; Botta, M.; Delli Castelli, D.; Fedeli, F.; Mortillaro, A.; Parker, D.; Puschmann, H. *Chem. Commun.* **2002**, 1120–1121. (c) Parker, D.; Puschmann, H.; Batsanov, A. S.; Senanayake, K. *Inorg. Chem.* **2003**, *42*, 8646–8651.

(20) Cotton, S. A.; Franckevicius, V.; Mahon, M. F.; Ooi, L. L.; Raithby, P. R.; Teat, S. J. *Polyhedron* **2006**, *25*, 1057–1068.

pyridine (62 mg) in 6 mL of MeOH gave 15 mg (43%) complex: mp >300 °C. Anal. Calcd for $C_{36}H_{32}N_7NdO_{10} \cdot MeOH \cdot H_2O$ ($M_r = 916.98$): C, 48.46; H, 4.18; N, 10.69. Found: C, 48.51; H, 4.03; N, 10.63.

Sm: Starting with $SmCl_3 \cdot 6H_2O$ (41 mg, 113 μ mol, 1.0 equiv), TREN-1,2-HOIQO·HCl·2H₂O·MeOH (92 mg, 113 μ mol, 1.0 equiv), pyridine (78 mg) in 20 mL of MeOH gave 61 mg (60%) complex: mp >300 °C. Anal. Calcd for $C_{36}H_{32}N_7O_{10}Sm \cdot MeOH$ ($M_r = 905.08$): C, 49.10; H, 4.01; N, 10.83. Found: C, 49.29; H, 3.99; N, 10.63.

Tb: Starting with $TbCl_3 \cdot 6H_2O$ (14.7 mg, 39.4 μ mol, 1.0 equiv), TREN-1,2-HOIQO·HCl·2H₂O·MeOH (32.0 mg, 39.4 μ mol, 1.0 equiv), pyridine (62 mg) in 6 mL of MeOH gave 16 mg (44%) complex: mp >300 °C. Anal. Calcd for $C_{36}H_{32}N_7O_{10}Tb \cdot MeOH$ ($M_r = 913.65$): C, 48.64; H, 3.97; N, 10.73. Found: C, 48.39; H, 4.06; N, 10.48.

Dy: Starting with $DyCl_3 \cdot 6H_2O$ (16.7 mg, 44.3 μ mol, 1.0 equiv), TREN-1,2-HOIQO·HCl·2H₂O·MeOH (36.0 mg, 44.3 μ mol, 1.0 equiv), pyridine (62 mg) in 6 mL of MeOH gave 23 mg (56%) complex: mp >300 °C. Anal. Calcd for $C_{36}H_{32}DyN_7O_{10} \cdot 2H_2O$ ($M_r = 921.21$): C, 46.94; H, 3.94; N, 10.64. Found: C, 46.74; H, 3.75; N, 10.45.

Ho: Starting with $HoCl_3 \cdot 6H_2O$ (14 mg, 38 μ mol, 1.0 equiv), TREN-1,2-HOIQO·HCl·2H₂O·MeOH (31 mg, 38 μ mol, 1.0 equiv), pyridine (62 mg) in 6 mL of MeOH gave 24 mg (69%) complex: mp >300 °C. Anal. Calcd for $C_{36}H_{32}HoN_7O_{10} \cdot MeOH$ ($M_r = 919.65$): C, 48.32; H, 3.95; N, 10.66. Found: C, 47.98; H, 3.99; N, 10.38.

Er: Starting with $ErCl_3 \cdot 6H_2O$ (10.4 mg, 38.2 μ mol, 1.0 equiv), TREN-1,2-HOIQO·HCl·2H₂O·MeOH (31.0 mg, 38.2 μ mol, 1.0 equiv), pyridine (62 mg) in 6 mL of MeOH gave 22 mg (62%) complex: mp >300 °C. Anal. Calcd for $C_{36}H_{32}ErN_7O_{10} \cdot MeOH$ ($M_r = 921.98$): C, 48.20; H, 3.94; N, 10.63. Found: C, 47.81; H, 4.06; N, 10.46.

Tm: Starting with anhydrous $TmCl_3$ (10.5 mg, 38.2 μ mol, 1.0 equiv), TREN-1,2-HOIQO·HCl·2H₂O·MeOH (31.0 mg, 38.2 μ mol, 1.0 equiv), pyridine (62 mg) in 6 mL of MeOH gave 20 mg (57%) complex: mp >300 °C. Anal. Calcd for $C_{36}H_{32}N_7O_{10}Tm \cdot MeOH$ ($M_r = 923.66$): C, 48.11; H, 3.93; N, 10.62. Found: C, 47.82; H, 4.02; N, 10.41.

Yb: Starting with $YbCl_3 \cdot 6H_2O$ (9.5 mg, 25 μ mol, 1.0 equiv), TREN-1,2-HOIQO·HCl·2H₂O·MeOH (20.0 mg, 25 μ mol, 1.0 equiv), pyridine (31 mg) in 5 mL of MeOH gave 13 mg (54%) complex: mp >300 °C. Anal. Calcd for $C_{36}H_{32}N_7O_{10}Yb \cdot 2MeOH \cdot H_2O$ ($M_r = 977.82$): C, 46.68; H, 4.33; N, 10.03. Found: C, 46.65; H, 3.89; N, 9.99.

4.3. Single-Crystal X-ray Analysis. Crystals were grown at room temperature by vapor diffusion of water into DMF solutions of the lanthanide complexes. Measurements for La–Yb (except Tm) were made on a Siemens SMART CCD²¹ area detector with graphite monochromated Mo K α radiation. The data for the structures of the

Tm and Lu complexes were collected at the Advanced Light Source (Lawrence Berkeley National Laboratory, Berkeley, CA) using monochromated synchrotron radiation ($\lambda = 0.7749$ Å). Data were integrated by the program SAINT²² and corrected for Lorentz and polarization effects. Data were analyzed for agreement and possible absorption using XPREP.²³ An empirical absorption correction based on the comparison of redundant and equivalent reflections was applied using SADABS.²⁴ Equivalent reflections were merged. No decay correction was applied. The structure was solved within the WinGX²⁵ package by direct methods (SIR92²⁶) and expanded using Fourier techniques (SHELXL-97²⁷). Hydrogen atoms (except for the two water molecules) were included but not refined. The hydrogen atoms of the water molecules could not unambiguously be assigned. Hydrogen atoms were positioned geometrically, with C–H = 0.93 Å for C_{arom}–H groups, C–H = 0.97 Å for CH₂ groups, and N–H = 0.89 Å and constrained to ride on their parent atoms. U_{iso}(H) values were set at 1.2 times U_{eq}(C) for all H atoms.

Acknowledgment. M.S. thanks the German Research Foundation (DFG) for a research fellowship. This work was supported in part by NIH Grant R01-HL69832 and by the Director, Office of Science, Office of Advanced Scientific Computing Research, Office of Basic Energy Sciences (U.S. Department of Energy) under contract DE-AC02-05CH11231. Data for the crystal structures of the Tm and Lu complexes were collected at Beamline 11.3.1 of the Advanced Light Source at Lawrence Berkeley National Laboratory operated under DOE Contract DE-AC03-76SF00098.

Supporting Information Available: CIF files for the crystal structures of all lanthanide complexes (except for Ce). Additional tables and diagrams for bond lengths and distances for the series [Ln(TREN-1,2-HOIQO)(H₂O)], [Ln(TREN-SAL)], [Ln(tpzt)(NO₃)₃(H₂O)], [Ln(PhMeCH-DOTAM)(H₂O)](OTf)₃, and [Ln(H₂O)₉](EtOSO₃)₃. This material is available free of charge via the Internet at <http://pubs.acs.org>.

JA072750F

(21) SMART, version 5.059: Area-Detector Software Package; Bruker Analytical X-ray Systems, Inc.: Madison, WI, 1999.

(22) SAINT, version 7.07B: SAX Area-Detector Integration Program; Siemens Industrial Automation, Inc.: Madison, WI, 2005.
 (23) XPREP, version 6.12: Part of the SHELXTL Crystal Structure Determination Package; Bruker AXS Inc.: Madison, WI, 1995.
 (24) Sheldrick, G. SADABS, version 2.10: Siemens Area Detector Absorption Correction Program; University of Göttingen: Göttingen, Germany, 2005.
 (25) WinGX 1.70.01: Farrugia, L. J. *J. Appl. Crystallogr.* **1999**, *32*, 837–838.
 (26) SIR92: Altomare, A.; Casciaro, G.; Giacovazzo, C.; Guagliardi, A. J. *Appl. Crystallogr.* **1993**, *26*, 343–350.
 (27) Sheldrick, G. M. SHELX97 - Programs for Crystal Structure Analysis; Institut für Anorganische Chemie der Universität: Göttingen, Germany, 1998.